An MPPT-Based ABC Algorithm Applied to PV Pumping Based BLDC Motor Drive under Partial Shading

Saliha Aoufi, Cherif Larbes, and Aissa Chouder

Abstract− In this paper, we propose a photovoltaic pumping system. Our system is composed of a photovoltaic generator, a boost converter (DC/DC) controlled by Maximum power point tracking (MPPT), an inverter (DC/AC), a motor-pump group (PMBLDC motor, centrifugal pump). The amount of energy produced by PV systems depends on environmental circumstances such as temperature and solar irradiance, the objective of our system is to ensure operation at a maximum power of the photovoltaic system, for this the Artificial Bee method Colony (ABC) was implemented. to evaluate the best and most accurate controller for different weather conditions. The results show that the use of the ABC method is effective and has an excellent performance in terms of response time and can increase the stability of the photovoltaic pumping system. The simulations of the different parts of the system are developed in the MATLAB/Simulink environment.

***Keywords*− Photovoltaic generator Maximum power point tracking. DC/DC chopper. DC-AC converter. PMBLDC motor. Centrifugal pump.**

NOMENCLATURE

ABC	Artificial Bee Colony
DC/DC	DC-DC converter
DC/AC	DC-AC converter
PMBLDC	Permanent magnet brushless direct current
MPPT	Maximum point tracking
PWM	Pulse Width Modulation
EMF	Electromotive force

I. INTRODUCTION

The generation of energy represents a major challenge for the coming years. The energy demands of industrialized nations continue to grow steadily, while developing countries will also require increasing amounts of energy to support their progress and modernization. Currently, a significant portion of global energy production relies on fossil fuels. However, the use of these resources leads to greenhouse gas emissions contributing to, environmental pollution. Moreover, the overconsumption of these non-renewable resources threatens to deplete natural reserves, posing serious risks for future generations [1].

In contrast, renewable energy sources offer a promising alternative, as they are both inexhaustible and can be harnessed in a more environmentally friendly and sustainable manner. A photovoltaic (PV) generator can operate over a wide range of voltage and current values. However, it can only deliver its maximum power at specific voltage and current levels, known as the Maximum Power Point (MPP). The position of this point is highly dependent on environmental conditions such as solar irradiance and temperature, which fluctuate continuously throughout the day [2]. These variations cause the MPP to shift, making it necessary to implement control strategies that can adapt in real-time without prior knowledge of the MPP location or the cause of its change. This control approach is commonly referred to as Maximum Power Point Tracking (MPPT).

Several MPPT techniques have been developed to optimize the performance of PV systems. Among the most widely used methods are the Perturb and Observe (P&O) algorithm, Fuzzy Logic Control, Artificial Neural Networks, and the Incremental Conductance Method [3]. The primary objective of these algorithms is to continuously track the MPP and ensure efficient energy transfer from the PV generator to the load, regardless of the external environmental changes.

This work aims to ensure optimal performance of the photovoltaic (PV) system under different climatic conditions.[4] To achieve this, we propose an MPPT control technique based on the Artificial Bee Colony (ABC) algorithm for maximum power extraction. The main contributions of this paper are: (i) the design of a new PV water pumping system, and (ii) the direct control of the system using ABC-based MPPT to improve efficiency.

The paper is structured as follows: first part presents the system architecture and modelling, second part describes the ABC algorithm, third part discusses simulation results, and concludes the study.

II. MANUSCRIPT PREPARATION GUIDELINES

Photovoltaic (PV) water pumping system is composed of several key components. It includes a PV generator formed by multiple interconnected solar modules that produce direct current (DC) power. A DC-DC converter is used to regulate the output voltage and frequency according to the available solar energy. Additionally, an inverter converts the DC power into alternating current (AC), while a Pulse Width Modulation (PWM) technique and an MPPT algorithm are implemented to optimize power extraction from the PV modules.

The system also includes a motor-pump assembly consisting of a PMBLDC motor coupled with a centrifugal pump.

Manuscript received April 9, 2026; accepted June 28, 2026.
Saliha Aoufi, Cherif Larbes, and Aissa Chouder are with the Electronics Department, Ecole Nationale Polytechnique, Algiers, ALGERIA (e-mail: Saliha.Aoufi@g.enp.edu.dz; Cherif.Larbes@g.enp.edu.dz; Aissa.Chouder@g.enp.edu.dz).

Digital Object Identifier (DOI): 10.53907/enpesj.v6i1.366

Figure 1 illustrates the overall structure of the proposed system.

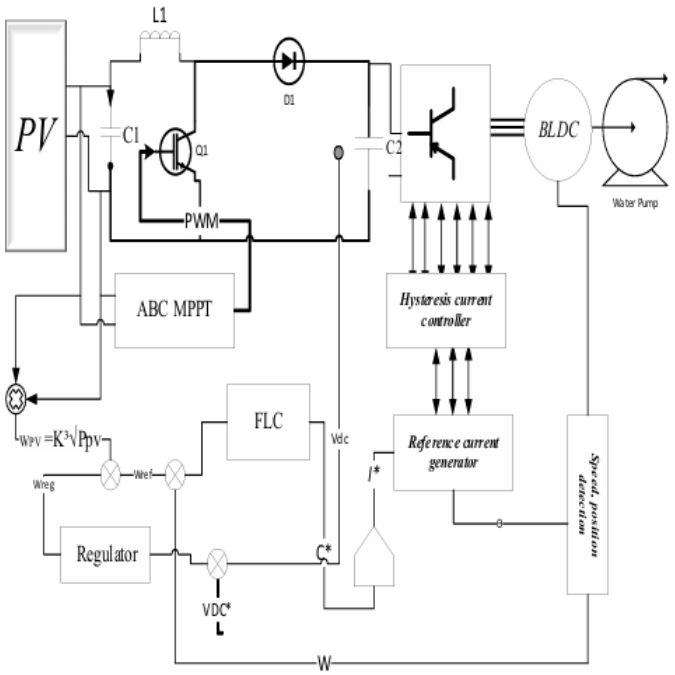

Fig. 1: Bloc Diagram of PV Pumping System

A. Modelling of PV pumping system

In existing literature, several circuit models have been proposed to represent the electrical characteristics of photovoltaic (PV) cells. However, in practical electrical engineering applications, only two models are predominantly used: the Single Diode Model (SDM) and the Double Diode Model (DDM) [5]. Among them, the SDM is most preferred in research due to its simpler structure and lower computational requirements compared to the DDM. The equivalent circuit of the SDM is shown in Figure 2.

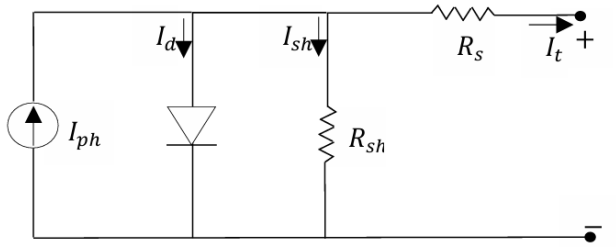

Fig. 2: PV cell equivalent circuit.

This model comprises a photo generated current source in parallel with a diode, a series resistor to denote the ohmic losses related to load current and a shunt resistor to present the leakage current [6]. Thus, in term of Kirchhoff's current law, the PV cell terminal current, it can be expressed by:

$$I_t = I_{ph} - I_d - I_{sh} \quad (1)$$

where Iph denotes the photo generated current, Id denotes the diode current, and Ish denotes the shunt resistor current, respectively.

Additionally, in term of Shockley equation, Id is computed by:

$$I_d = I_{sd}\left[\left(\exp\left(\frac{q(V_t + I_t R_s)}{akT}\right) - 1\right)\right] \quad (2)$$

where Isd is the reverse saturation current of diode, Vt is the cell terminal voltage, Rs is the series resistance, a is the diode factor, k is the Boltzmann constant (1.380 × 10−23 J/K), q is the electronic charge (1.602 × 10−19 C), and T is the PV cell absolute temperature in Kelvin, respectively.

Moreover, using Kirchhoff's voltage law, Ish is obtained as:

$$I_{sh} = \frac{(V_t + I_t R_s)}{R_{sh}} \quad (3)$$

where Rsh is the shunt resistance.

Therefore, by substituting from Equations (2) and (3) into Equation (1), the I-V relationship of the SDM can be rewritten as follows:

$$I_t = I_{ph} - I_{sd}\left[\left(\exp\left(\frac{q(V_t + I_t R_s)}{akT}\right) - 1\right)\right] - \frac{(V_t + I_t R_s)}{R_{sh}}$$

The specifications of the PV module are given in Table 1

Table 1: PV module parameters

Pmax	Vmp	Imp	Voc	Isc
280	37.01	7.57	43.9	8.14

B. Design of Boost Converter

An energy converter plays a critical role in photovoltaic (PV) systems by serving as an interface between the PV array and the load. Typically, a DC-DC converter is used for this purpose, functioning as a Maximum Power Point Tracker (MPPT). It dynamically adjusts the output voltage of the PV generator to ensure that the system operates at its maximum power point under varying levels of solar irradiance and ambient temperature [7]. This is achieved by controlling the duty cycle of the converter, which regulates the power flow. One of the most used types is the boost converter, also known as a step-up or parallel chopper, which increases the DC voltage from the PV source to a higher level suitable for the load or subsequent stages of the system.

The variation in voltage across the capacitor (output voltage ripple of the Boost converter) is expressed by the following relationship:

$$\Delta V_{c2} = \Delta V_{dc} = \frac{V_{pv}}{R_s C_2 f_p}\frac{D}{1-D}$$

The fictitious load resistance Rs relates the output voltage to the output current in a boost converter. Because this converter maintains power balance (input power equals output power), Rs also reflects the input voltage to input current ratio. To size the output capacitor C2 for the nominal maximum power point of a photovoltaic system (1000 W/m² at 25 °C), Rs is defined based on specific input voltage and current values.

$$R_s = \frac{V_{c2}}{I_2} = \frac{V_{dc}}{I_2} = \frac{V_{pv}}{I_2} = \frac{V_{mp}}{I_2}$$

The output voltage ripple of a Boost converter depends on system parameters and the duty cycle D. As D increases, the amplitude of the ripple also increases. To size the capacitor C, it is advisable to consider a worst-case scenario by using the maximum value of D, which may lead to over-sizing C if the operation occurs at a lower D.

Additionally, selecting a high switching frequency f is

preferable to reduce the required capacitance of the capacitor. Assuming a linear variation of the current in the inductor, this variation or ripple of the current is given by:

$$\Delta I_e = \frac{U_{ei}}{L_e f} D$$

The current ripple is directly proportional to the duty cycle D.

To size the inductance L, the maximum D should be considered to keep the ripple within limits. Choosing a high switching frequency fp also helps reduce the required inductance and limit the ripple. The variation in voltage across the input capacitor C1 is expressed by:

$$\Delta \mathrm{V_{c1}} = \frac{\Delta I_1}{8 f_p C_1}; \quad C_1 = \frac{\Delta I_1}{8 f_p \Delta_{c1}}$$

The amplitude of the input voltage variation (ΔVin) is proportional to the current ripple in the input inductor (ΔIl) and inversely proportional to the capacitor value C1 and the switching frequency (fp). To limit (ΔVin), one can increase the input capacitor C1or the switching frequency (fp).

C. Modelling of the BLDC Motor Drive System

Theoretically, PMBLDC (Permanent Magnet Brushless DC) and AC machines share operational principles with conventional DC machines; however, they replace the mechanical collector with an electronic commutator. This transition enhances efficiency and reduces maintenance needs. In the context of conventional DC generators connected in parallel to a DC network, BLDC motors exhibit a superior torque-to-size ratio, making them particularly valuable in applications where space and weight constraints are critical, such as aerospace, robotics, and portable electronics [8].

Moreover, BLDC motors are designed to generate trapezoidal waveform electromotive forces (EMFs) while being supplied with rectangular stator currents. This configuration not only helps achieve a consistent torque output but also improves overall efficiency and performance. Additionally, the precise control of these motors allows for rapid response times and smooth operation, making them suitable for high-performance applications. The electronic commutation also enables advanced control strategies, such as field-oriented control, which further optimize their performance under dynamic conditions [9].

Table 2: Six step switching sequence for commutation

Rotor position	H1	H2	H3	Switch Closed	Phase current		
					A	B	C
0-60	1	0	0	S1 S4	+	-	0
60-120	1	1	0	S1 S6	+	0	-
120-180	0	1	0	S3 S6	0	+	-
180-240	0	1	1	S3 S2	-	+	0
240-300	0	0	1	S5 S2	-	0	+
300-360	1	0	1	S5 S4	0	-	+

The BLDC motor's uniqueness stems from its trapezoidal electromotive force, resulting in non-sinusoidal mutual inductance between the stator and rotor. The parameter, $\varphi 0$, is the magnitude of the magnetic flux created by the permanent magnet and the electrical angle. Thus, it yields

$$\vec{V} = [R]\vec{I} + \frac{d}{dt}\{[L]\vec{I}\} + \frac{d}{dt}\overrightarrow{\varphi_M}$$

where V and I are vectors representing voltage, current respectively for each phase, φM is the vector of the magnetic flux created by the permanent magnet, $[R]$ et $[L]$ are the resistance and inductance matrices of the machine.

For a symmetrical three-phase winding and a balanced system, the vector of the voltages at the terminals of the three phases is given by:

$$\begin{pmatrix} v_a \\ v_b \\ v_c \end{pmatrix} = \begin{pmatrix} R & 0 & 0 \\ 0 & R & 0 \\ 0 & 0 & R \end{pmatrix} \begin{pmatrix} i_a \\ i_b \\ i_c \end{pmatrix} + \frac{d}{dt} \begin{pmatrix} L_{aa} & L_{ab} & L_{ac} \\ L_{ba} & L_{bb} & L_{bc} \\ L_{ca} & L_{cb} & L_{cc} \end{pmatrix} \begin{pmatrix} i_a \\ i_b \\ i_c \end{pmatrix} + \begin{pmatrix} e_a \\ e_b \\ e_c \end{pmatrix}$$

with e represents the electromotive force.

The mechanical model of the BLDC motor is given by:

$$\frac{Jd}{dt} w_r = C_e - f w_r - C_r$$

where wr is the angular velocity, in rad/s, Ce is the electromagnetic torque N/m, Cr is the load torque N/m and f is the coefficient of friction on $N.(m/\,rad).s{-}1$.

To generate trapezoidal currents in the machine windings, a 120° control strategy with a single hysteresis regulator is employed. This method uses a hysteresis band around the reference current to control transistor signals based on the measured current's intersection with the band limits. It is cost-effective, requiring a 6-sector position sensor and one or two current sensors. The operation is divided into six 60° sectors, activating only two machine phases at a time, except during switching [10]. The magnitude of the phase current (I*) is determined from the reference torque: I* = C* / K. Depending on the position of the rotor, the reference current generator block produces three phase currents (IA*, IB*, IC*) by assigning the reference current values (I*, −I*, and zero).

D. Modelling of the Pump

The Q-H curve represents the relationship between lift height and discharge, with manufacturers providing maximum and minimum curves based on wheel diameter. A centrifugal pump operates with three key parameters: height, flow, and speed. [28] Using the motor's rotational speed as a parameter, the "PELEIDER-PETERMAN" model is expressed as follows:

$$H_n = a_1 w^2 + a_2 wq + a_3 q^2$$

in which, a1, a2 and a3 are geometric parameters characterizing the pump. It should be noted that the other expression to consider is that of the power in Watts absorbed by a pump, i.e. the power required for its mechanical drive, which is expressed by:

$$P = 9.81 \frac{QH}{n_p}$$

The pump efficiency is defined as the ratio of the hydraulic power imparted by the pump to the fluid to the shaft mechanical power [11].

III. MPPT Control Techniques for PV System

A. Artificial Bee Colony

The ABC algorithm is a population-based, iterative optimization technique modelled after the intelligent foraging behaviour of honeybees. It consists of three main types of bees [12]:

- Employed Bees: Search for food sources (possible solutions) and share the information with onlooker bees.
- Onlooker Bees: Select food sources based on the quality (fitness) shared by employed bees and then further exploit the most promising ones.
- Scout Bees: Explore the environment randomly to find new food sources (diversify the search to avoid local maxima).

The flowchart of the ABC algorithm is given in Figure 3.

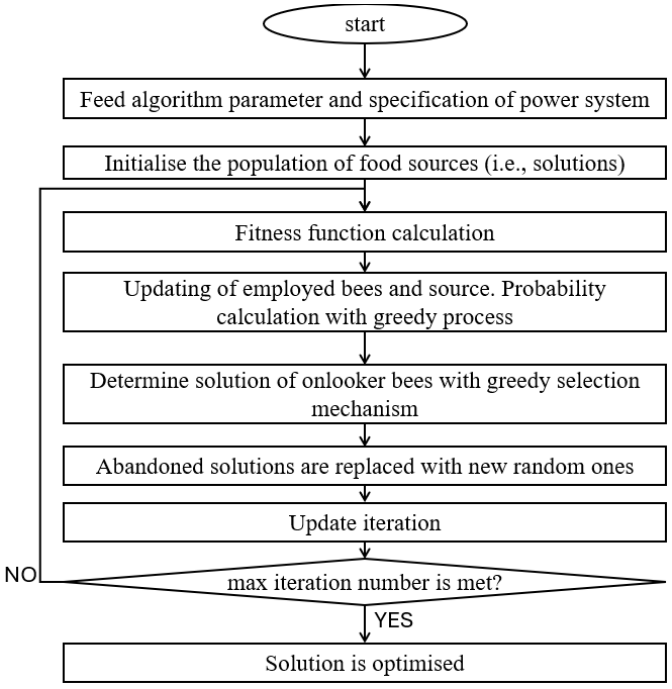

Fig. 3: Flowchart of ABC algorithm.

As can be seen in this figure, the process is as follows:

1. Initialization

Parameters Setup: Define the number of solutions SN (duty cycles), maximum cycle number MCN, and sampling time Ts, ensuring Ts exceeds the power converter's settling time.

Initial Population: Generate a randomly distributed initial population of solutions (duty cycles) within the range [0, 1].

2. Employed Bees Phase

Solution Update: Each employed bee modifies its current solution by exploring a neighbouring solution, aiming to improve its fitness.

Evaluation: Calculate the fitness of the new solution. •

Greedy Selection: If the new solution is better, update the current solution; otherwise, retain the existing one.

$$d_i = d_{min} + \text{rand}[0,1][d_{max} - d_{min}]$$

3. Onlooker Bees Phase

Probability Calculation: Determine the probability of selecting each solution based on its fitness.

Solution Selection: Onlooker bees probabilistically select solutions and explore their neighbourhoods.

Evaluation and Selection: Evaluate the new solutions and apply greedy selection as in the employed bee's phase.

4. Scout Bees Phase

Exploration: Scout bees randomly generate new solutions to replace those that are stagnated or less fit.

Evaluation: Assess the fitness of the new solutions.

Update: Replace the old solutions with the new ones if they are better as below

$$new(d_i) = d_i + \Phi_i(d_i - d_j)$$

5. Repeat

Repeat the above phases until the maximum cycle number MCN is reached or the power value remains unchanged within a specified number of cycles.

B. Effect of Irregular Solar Radiation

The PV generator, which consists of five modules connected in series, is subjected to various forms of solar irradiation, including uniform and non-uniform (partial shading), as shown in Table 4, in order to examine the behaviour of the chosen PV pumping system. Three modes of sunlight are in fact taken into consideration: two distinct non-uniform modes of sunlight and a uniform mode of sunlight (case 2). (Participatory appeal of Cases 1 and 3. 4).

Table 3: Solar irradiation modes (W/m2) for each module of the PV system

CASE 1	CASE 2	CASE 3	CASE 4
1000	800	1000	800
1000	800	1000	800
1000	800	1000	600
1000	700	1000	600
900	800	1000	1000
800	600	800	800
800	600	1000	1000

To evaluate the performance of the PV system under different irradiance conditions, the power-voltage (P–V) and current-voltage (I–V) characteristics of the PV array were analysed. Figure 4 presents the obtained characteristics for both uniform irradiance and partial shading conditions, highlighting the location of the maximum power points (MPPs) under each operating scenario. The figure clearly shows the existence of a single MPP under uniform irradiance and multiple local MPPs under partial shading conditions.

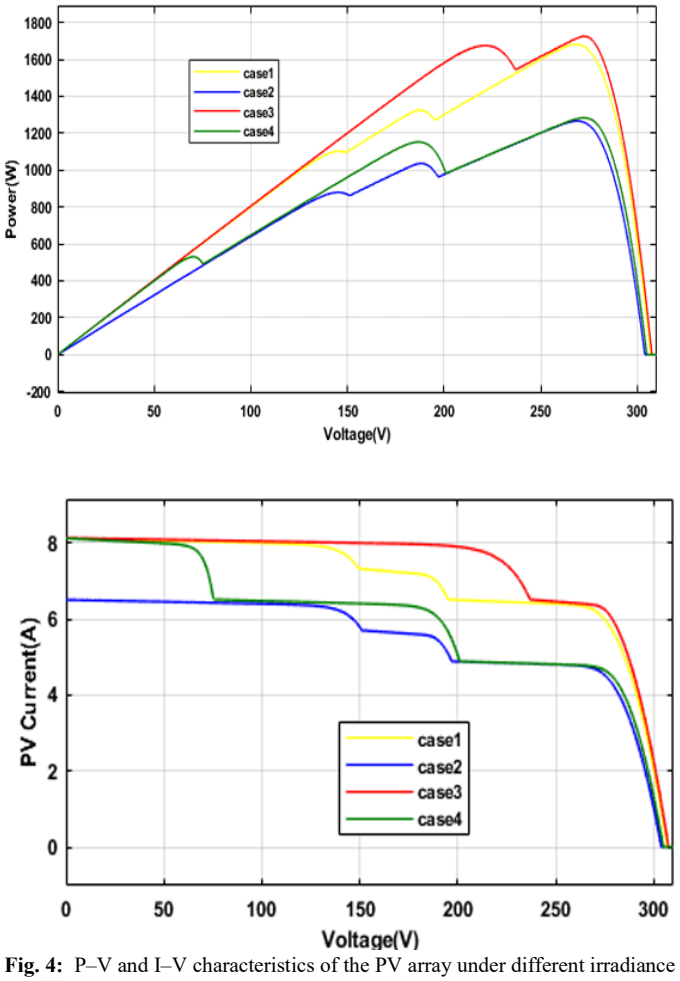

Fig. 4: P–V and I–V characteristics of the PV array under different irradiance conditions.

The uniform irradiance condition of Case 1 is characterized by the presence of a single maximum power point (MPP), with a power output of 1682 W corresponding to a PV generator voltage of 251 V and a current of 6.7 A (Figure 4).

The partial shading condition of Case 2 is characterized by the presence of three local maximum power points and one global maximum power point. The global maximum power achieved under this condition is 1265 W, corresponding to a PV generator voltage of 268 V and a current of 4.8 A (Figure 4).

Based on these observations, controlling the output voltage of the PV generator is essential to ensure operation at the maximum power point under varying temperature and irradiance conditions. This improves both the power conversion efficiency of the PV generator and the overall system performance. To achieve this objective, the MPPT-ABC algorithm is employed, which has demonstrated fast convergence and reliable performance when applied to the PV generator–Boost converter system.

To assess the effectiveness of the proposed ABC-MPPT algorithm, the dynamic responses of the PV power, PV current, and PV voltage were monitored under different irradiance conditions. The corresponding simulation results are presented in Figure 5.

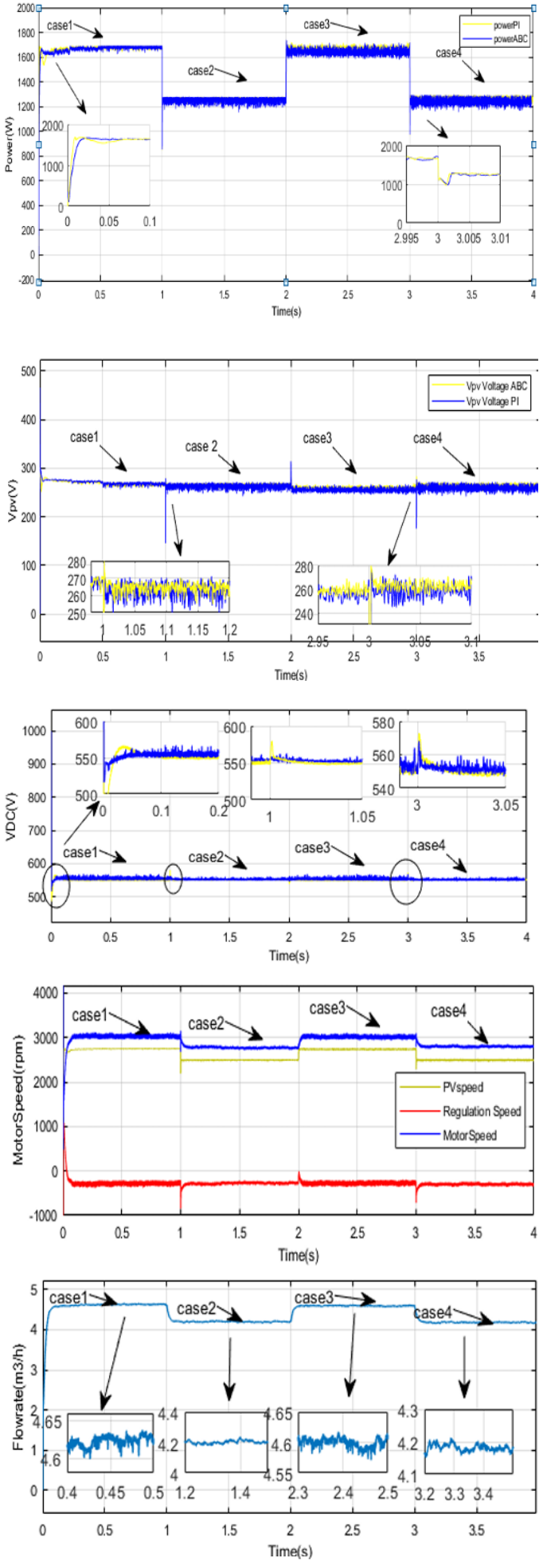

Fig. 5: Dynamic response of the ABC-MPPT algorithm: (a) PV output power, (b) PV array current, and (c) PV array voltage.

Under the first irradiance condition (Case 1), the ABC-MPPT algorithm achieved a steady-state PV power of approximately 1678 W after a response time of 0.02 s (Figure 5a). This corresponds to an efficiency of 99.71% relative to the theoretical maximum power of 1682 W shown in Figure 4.

The voltage across the PV array was measured at 260 V, while the current reached 6.3 A (Figures 5b and 5c). These values are very close to the reference maximum power point values of 261 V and 6.5 A, respectively (Figure 4). In this case, the duty cycle stabilized at 0.4033. The corresponding load voltage and current are illustrated in Figures 5c and 5b, respectively.

Under the second irradiance condition (Case 2), the steady-state PV power reached approximately 1260 W after a response time of 0.01 s (Figure 5a). The ABC-MPPT algorithm maintained an efficiency of 99.6% relative to the theoretical maximum power of 1265 W (Figure 4). The PV array voltage was 261 V, while the current was 4.7 A (Figures 5c and 5b).

Similar results were obtained for the partial shading conditions of Cases 3 and 4. The ABC-MPPT algorithm enabled the PV array to reach 99.83% of its actual global maximum power. The corresponding output powers were approximately 1721 W and 1283 W for Cases 3 and 4, respectively (Figure 5a). The system response time was approximately 0.01 s. The PV array voltage was measured at 257 V, while the current reached 3.3 A (Figures 5c and 5b), which are very close to the reference maximum power point values of 251 V and 3.39 A.

These results demonstrate that, under different irradiance conditions, the ABC-MPPT algorithm is capable of accurately tracking the global maximum power point with high efficiency, fast response, and excellent stability.

C. Efficiency Estimation of BLDC Motor–Pump System

A very good efficiency is obtained for the proposed water pumping system. Table 7 and Figure7. show the efficiency estimation of the BLDC motor-pump system and its graphical representation respectively, subjected to the variation in atmospheric condition, we present the variations in the water flow rate of the pump (Q) and power with irradiation variation.

As the solar insolation level changes, various indices of the BLDC motor-pump system, such as back EMF (ea), stator current (isa), speed (W), electromagnetic torque, and load torque, also vary in response to the solar insolation, as illustrated in les Figures precedent. Two key observations can be drawn from the simulation results. First, the stator current (isa) is controlled during startup, allowing it to gradually reach its steady-state value, resulting in a soft start for the BLDC motor. Second, the electromagnetic torque generated by the BLDC motor consistently matches the torque required to drive the pump, demonstrating the system's stable operation under varying solar insolation conditions, regardless of whether fluctuations.

In the solar pumping system without energy storage, all the electricity produced by the photovoltaic generator (Ppv) is directly used by the pump motor (Pm). It is essential to maintain a constant balance between Ppv and Pm to prevent any instability in the system. This requires controlling the rotational speed of the pump motor, which must correlate with the mechanical power (Pm) of the motor to align with the photovoltaic power (Ppv). Thus, the reference speed is calculated based on Ppv. In parallel, a regulation speed is introduced, with an opposite sign to Wpv, to obtain the total reference speed This regulation speed allows for the control of the charge and discharge power of the bus capacitor, ensuring that the voltage remains close to its reference value.

Table 4: Parameters of BOOST and BLDC motor

PARAMETER	VALUE	PARAMETER	VALUE
Boost		**BLDC**	
L (mH)	5.7	Stator phase resistance (Ω)	2.875
C1 (µF)	1.728	Stator phase inductance (mH)	8.5
C2 (µF)	57.51	Flux linkage (V.s)	0.175
f (kHz)	50	Inertia ($kg.m^2$)	8e-4
		Viscous damping (N. ms)	e-3
		Pole pair	4

A. CONCLUSION

This study focused on modelling and analysing the components of a photovoltaic (PV) water pumping system, which includes an BLDC motor pump powered by a PV generator through a BOOST converter and an inverter. An analysis was conducted on Maximum Power Point Tracking (MPPT) technique: the ABC (Artificial Bee Colony. Among these, the algorithm demonstrated superior performance, maintaining consistent operation at maximum power with rapid and accurate tracking even under changing weather conditions. Its robustness was verified under various solar radiation scenarios. The results revealed that the ABC method outperformed the other two in terms of response time, resistance to climate variation, and water flow efficiency. Moreover, it enabled effective operation even at very low solar irradiance levels.

Overall, the proposed system significantly enhances the efficiency of PV-based water pumping. Future work will explore the integration of hybrid optimization algorithms for broader photovoltaic applications.

REFERENCES

[1] M. B. Jebli and M. Kahia, “The interdependence between CO2 emissions, economic growth, renewable and non-renewable energies, and service development: Evidence from 65 countries,” Climate Change, vol. 162, no. 2, pp. 193–212, 2020.

[2] J. Shi, W. Zhang, Y. Zhang, F. Xue, and T. Yang, “MPPT for PV systems based on a dormant PSO algorithm,” Electric Power Systems Research, vol. 123, pp. 100–107, 2015.

[3] Z. Zhao, R. Cheng, B. Yan, J. Zhang, Z.-H. Zhang, M. Zhang, and L. L. Lai, “A dynamic particle MPPT method for photovoltaic systems under partial shading conditions,” Energy Conversion and Management, vol. 220, 2020.

[4] G. Li, Y. Jin, M. W. Akram, X. Chen, and J. Jia, “Application of bio-inspired algorithms in maximum power point tracking for PV systems under partial shading conditions—A review,” Renewable and Sustainable Energy Reviews, vol. 81, pp. 840–873, 2018.

[5] A. A. S. Mohamed, A. Berzoy, and O. Mohammed, “Design and hardware implementation of FL-MPPT control of PV systems based on GA and small-signal analysis,” IEEE Transactions on Sustainable Energy, vol. 8, no. 1, pp. 279–290, Jan. 2017.

[6] M. V. da Rocha, L. P. Sampaio, and S. A. O. da Silva, “Comparative analysis of MPPT algorithms based on Bat algorithm for PV systems under partial shading conditions,” Sustainable Energy Technologies and Assessments, vol. 40, Art. no. 100761, 2020.

[7] A. Ahmed and Z. Salam, “An improved perturb and observe (P&O) maximum power point tracking (MPPT) algorithm for higher efficiency,” Applied Energy, vol. 150, pp. 97–108, 2015.

[8] R. Kumar and B. Singh, “BLDC motor driven solar PV array fed water pumping system employing Zeta converter,” IEEE Transactions on Industry Applications, doi: 10.1109/TIA.2016.2522943.

[9] H. B. Hansen, C. S. K. Kallesøe, and J. D. Bendtsen, "A hybrid model of a brushless DC motor," in Proc. 16th IEEE International Conference on Control Applications, 2007.

[10] A. Terki, A. Moussi, A. Betka, and N. Terki, "An improved efficiency fuzzy logic control of PMBLDC for PV pumping systems," Mathematical Modelling, vol. 36, pp. 934–944, 2012.

[11] S. Meunier, M. Heinrich, L. Quéval, J. A. Chernic, L. Vido, et al., "A validated model of a photovoltaic water pumping system for off-grid rural communities," Applied Energy, vol. 241, pp. 580–591, 2019.

[12] X. Bi and Y. Wang, "Artificial bee colony algorithm with fast convergence," Systems Engineering and Electronics, vol. 33, no. 12, pp. 2755–2761, 2011.